Silicon (2018) 10:981–993
DOI 10.1007/s12633-017-9556-7

ORIGINAL PAPER

Synthesis and Structural Characterization of G-SBA-IDA, G-SBA-EDTA and G-SBA-DTPA Modified Mesoporous SBA-15 Silica and Their Application for Removal of Toxic Metal Ions Pollutants

Issa M. El-Nahhal[1] · Mohamed Chehimi[2] · Mohamed Selmane[3]

Received: 1 May 2016 / Accepted: 3 February 2017 / Published online: 28 June 2017

Abstract Modified mesoporous SBA-15 silica materials (G-SBA-IDA, G-SBA-EDTA and G-SBA-DTPA) (where IDA, EDTA and DTPA represent iminodiacetic acid, ethylenediaminetetraacetic acid and diethylenetriaminepentaacetic acid, respectively) were prepared by treatment of grafted monoamine or diamine or triamine mesoporous SBA-15 silica (G-SBA-N, G-SBA-NN, G-SBA-NNN) nanomaterials with ethylchloroacetate, followed by acid hydrolysis of ester groups. These materials were characterized by several techniques including transmission electron microscopy (TEM), scanning electron microscopy (SEM) with energy dispersive X-ray spectroscopy (EDS), Fourier transform infrared spectroscopy (FTIR), small angle X-ray scattering (SAXS), thermal analysis (TGA) and X-ray photoelectron spectroscopy (XPS). TEM and BET analysis revealed that the IDA functionalized amine mesoporous SBA-15 silica materials have maintained their mesostructure after modification of the amine mesoporous silica with ethylchloroacetate. Thermal analysis (TGA-DTA) and FTIR confirmed that ethylchloroacetate groups are covalently bound to the amine groups. The acid forms of IDA functionalized materials showed high potential for extraction and removal of heavy pollutant metal ions (Co^{2+}, Ni^{2+}, $Cu^{2+}$and Pb^{2+}) from aqueous solutions.

Keywords SBA-15 mesoporous silica · Modified SBA-15 silica · Mesoporous silica nanoparticles · Sol-gel process · IDA-grafted mesoporous SBA-15 silica

1 Introduction

A great deal of research has been directed towards functionalized mesoporous SBA-15 silica, not only associated with structure features but also due to essential enormous potential applications in many different areas. The SBA type silica was first synthesized using a nonionic block polymer as a template [1]. These materials were prepared at low pH, where interaction between silica precursor and template through Si-OH + X^-H^+ is expected. SBA-15 mesoporous silica is generally obtained through the reaction of template pluronic acid 123 under acidic condition. A lot of research work has been directed to the synthesis of well-defined hybrid organic-inorganic silica based porous materials, because of their fascinating regular mesostructure along with high specific surface area, thermal and mechanical stability, uniform pore distribution and high adsorption capacity [2–6]. There are two different methods reported for preparation of functionalized mesoporous silica [7, 8], the co-condensation method in which the functional groups are introduced into the interior channel of the pore side and the grafting method (post-synthesis) in which

✉ Issa M. El-Nahhal
issanahhal@hotmail.com

[1] Department of Chemistry, Al-Azhar University, P O Box 1277, Gaza, Palestine

[2] ITODYS Laboratory § Leader of the Surface & Interface Research Team Université Paris Diderot -CNRS (UMR 7086), 15 rue Jean de Baïf, 75013 Paris, France

[3] Laboratoire de Chimie de la Matière Condensée de Paris, Université Piere, Curie-Paris 6, CNRS, College de France, 11 place Marcelin Berthelot, Paris 75231, France

the functional groups are introduced into the external side of the pore. There is a significant potential of work for synthesis of functionalized amine and other ligand systems, because of their versatile applications [9–12]. Iminodiacetic acid(IDA)-functionalized mesoporous materials are very interesting, because they have a wide range of applications in drug delivery [13], adsorption, separation and removal of toxic heavy metal ions from water [14–21], environmental studies [17–21] and biochemistry [21]. Most previous reported work was concerned with IDA-functionalized silica or modification of pre-prepared functionalized polysiloxane materials. Few research articles are reported on synthesis of IDA-modified mesoporous silica [13, 17, 22]. Iminodiacetic acid (IDA), ethylenediaminetetraacetic acid (EDTA) and diethylenetriaminepentaacetic acid (DTPA) have favorable chelating groups and ion-exchange properties for many different metal ions. Therefore, their immobilization onto inorganic mesoporous SBA-15 silica supporting materials, for metal adsorption purposes should receive wide attention. The reasons for selecting the following materials G-SBA-IDA, G-SBA-EDTA and G-SBA-DTPA, are the parent substrate SBA-15 silica has higher surface area, large wall thickness and it is thermally and mechanically stable. These materials would also have a wide range of applications in environmental and biochemical fields.

In this research article, three modified mesoporous SBA-15 silica ligand systems namely IDA-, EDTA- and DTPA- were prepared via modification of grafted monoamine, diamine and triamine mesoporous materials with ethylchloroacetate followed by hydrolysis using HCl. Their potential for extraction and removal of some heavy toxic metal ions (Co^{2+}, Ni^{2+}, $Cu^{2+}$and Pb^{2+}) from aqueous solutions was examined and compared with the data of reported similar IDA- and EDTA-functionalized polysiloxane ligand systems. These materials have promising application for removal of toxic heavy metals. Several techniques were used for the structure characterization of these new materials. These methods include: X-ray photoelectron spectroscopy (XPS), transmission electron microscopy (TEM), scanning electron microscopy (SEM-EDS), Fourier transform infrared spectroscopy (FTIR), small angle X-ray scattering (SAXS), and thermal analysis (TGA).

2 Materials and Methods

2.1 Materials

Tetraethylorthosilicate, ethylchloroacetate, iminodiacetic acid (IDA) and pluronic P123 ($EO_{20}PO_{70}EO_{20}$), were purchased from (Merck) and used as received. The organoalkoxysilanes selected for the functionalization process were 3-aminopropyltrimethoxysilane [1-(2-aminoethyl)-3-aminopropyl] trimethoxysilane and 1-[3-(trimethoxysilyl)-propyl]-diethylenetriamine. These reagents were purchased from the Aldrich company and used without further purification. Toluene and ethanol (spectroscopic grade) were purchased from Aldrich and used as received. Metal ion solutions of the appropriate concentration were prepared by dissolving the metal nitrate (analar grade) in deionized water.

2.2 General Techniques

Infrared spectra for the materials were recorded on a Perkin-Elmer FTIR, spectrometer using a KBr disk in the range 4000 to 400 cm^{-1}. All pH measurements were obtained using an AD1020 pH Meter. All ligand samples were shaken with aqueous metal ion solutions using an ELEIA-Multi Shaker. The concentrations of metal ions in their aqueous solutions were measured using a Perkin-Elmer AAnalyst-100, spectrometer.

Thermogravemetric analysis TGA was carried out for the samples using a Mettler Toledo SW 7.01 analyzer in the range of 25-600 ^{o}C under nitrogen. Scanning electron microscopy (SEM) was performed with a Philips X130 ESEMFEG with energy dispersive X-ray (EDS) spectroscopy. The transmission electron microscopy (TEM) analysis was done with a Tecnai F300 transmission electron microscope, with images taken after suspending the nanoparticles in ethanol. N_2 adsorption–desorption isotherms at 77K were measured by using a Micromeritics Tristar 3000 sorptometer to determine textural properties. Surface area was calculated by using the BET equation.

XPS spectra were recorded using a K Alpha (Thermo) fitted monochromatic Al K X-ray source (spot size: 400 μm). The pass energy was set to 200 and 50 eV for the survey and the narrow regions, respectively. The spectra were calibrated against the C-C/C-H C1s component set at 285 eV. The composition was determined using the manufacturer's sensitivity factors.

2.3 Preparations

2.3.1 Preparation of SBA-15 Silica Nanoparticles

SBA-15 pure silica was prepared by using pluronic P123 triblock copolymer as previously prepared [1]. 4.0 g of P123 was dissolved at room temperature in 125 ml 2M HCl. TEOS was added to the solution and stirred at 35 °C for 24 h, then autoclaved at 100 °C in a sealed reactor at 100 °C for 48 h. The solid product was isolated by filtration and washed with water and ethanol. The surfactant was removed

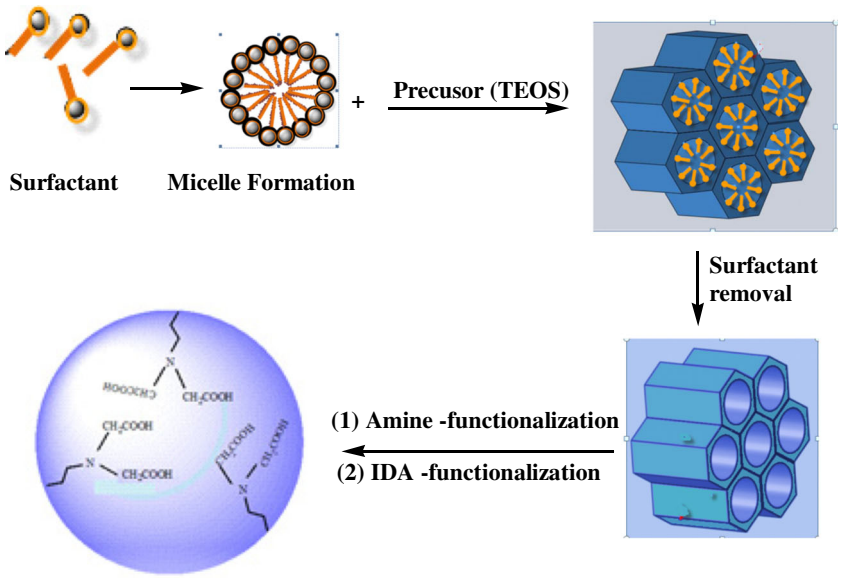

Scheme 1 Systematic drawing of the formation of IDA-functionalized mesoporous SBA-15 silica

using two ways, by reflux in ethanol or calcination at 600 °C for four hours.

2.3.2 Preparation of Amine Functionalized Silica Mesoporous Nanoparticles

Amine functionalized mesoporous material was prepared as previously described [8, 23] by dispersing 1.0 g of the pure silica SBA-15 (surfactant was washed by ethanol) and the appropriate amount (0.02 mol) of amine silane coupling agent precursor in 30 ml of dry toluene. The mixture was refluxed for 24 h at 110 °C. The solid material was filtered off, washed with toluene and ethanol and dried in vacuum at 60 °C for 24 h. The products are labeled as G-SBA-N, G-SBA-NN and G-SBA-NNN for grafted monoamine-, diamine- and triamine-mesoporous SBA-15 silica, respectively.

Preparation of mesoporous Silica G-SBA-IDA, G-SBA-EDTA and G-SBA-DTPA G-SBA-IDA, G-SBA-EDTA and G-SBA-DTPA mesoporous silica materials were prepared by modification of grafted amine mesoporous SBA-15 silica materials G-SBA-N, G-SBA-NN and G-SBA-NNN, with excess of ethylchloroacetate as follows: 1.0 g

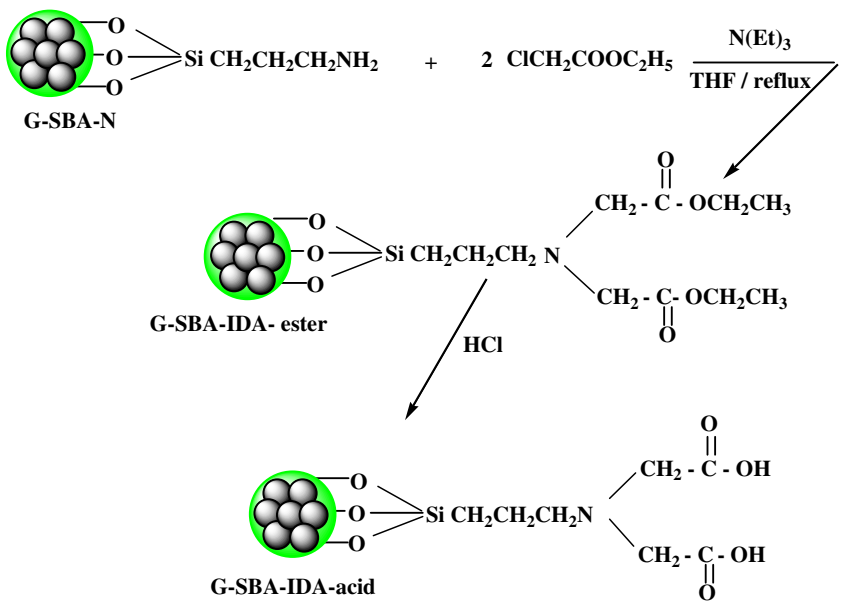

Scheme 2 Synthesis of G-SBA-IDA

Scheme 3 Synthesis of G-SBA-EDTA

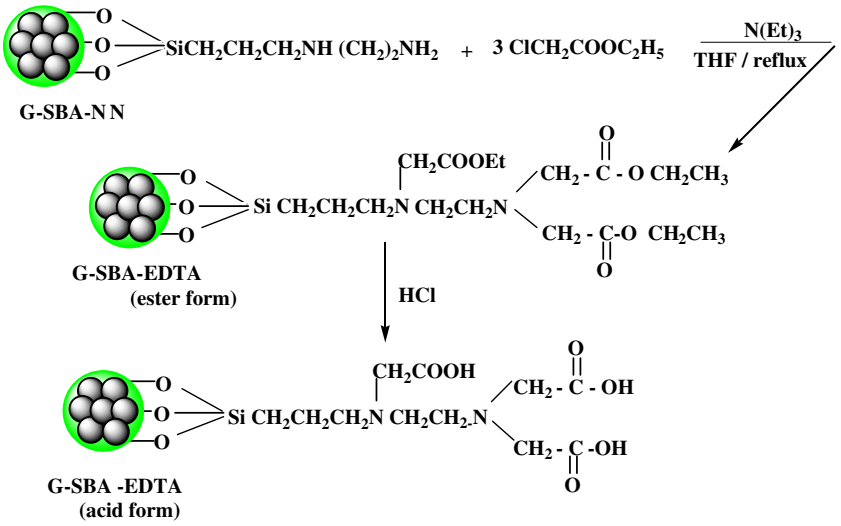

of functionalized grafted amine material was refluxed with excess of ethylchloroacetate in ethanol at 80 °C for 48 h. The products labeled as G-SBA-IDA, G-SBA-EDTA and G-SBA-DTPA materials were filtered and washed with ethanol three times. They were dried in vacuum at 60 °C for 48 h, and hydrolyzed using 2M hydrochloric acid at 90 °C for 8 h.

2.3.3 Metal Uptake Experiments

50 mg each of G-SBA-IDA or G-SBA-EDTA or G-SBA-DTPA-modified mesoporous SBA-15 silica material (acid form) was shaken with 50 ml, of 0.02 M of aqueous solution of the appropriate metal ions (Co^{2+}, Ni^{2+}, Cu^{2+} and Pb^{2+}) using 100 ml glass conical flasks for 48 h. Determination of the metal ion concentration was carried out by allowing the insoluble complex to settle and an appropriate volume of the supernatant was withdrawn using a micropipette then diluted to the linear range of the calibration curve for each metal. The metal ion uptake was calculated as mmole of M^{2+}/g ligand. Each study was performed at least in triplicate. Metal uptake was examined. The metal uptake capacity experiments for each of the three ligand systems was conducted in the same way, by treatment of a certain amount of the ligand system for 48 hours under shaking with an aqueous solution of the metal ion, an excess of metal ions was used to ensure the equilibrium state between metal ions and immobilized ligand.

Scheme 4 Synthesis of G-SBA-DTPA

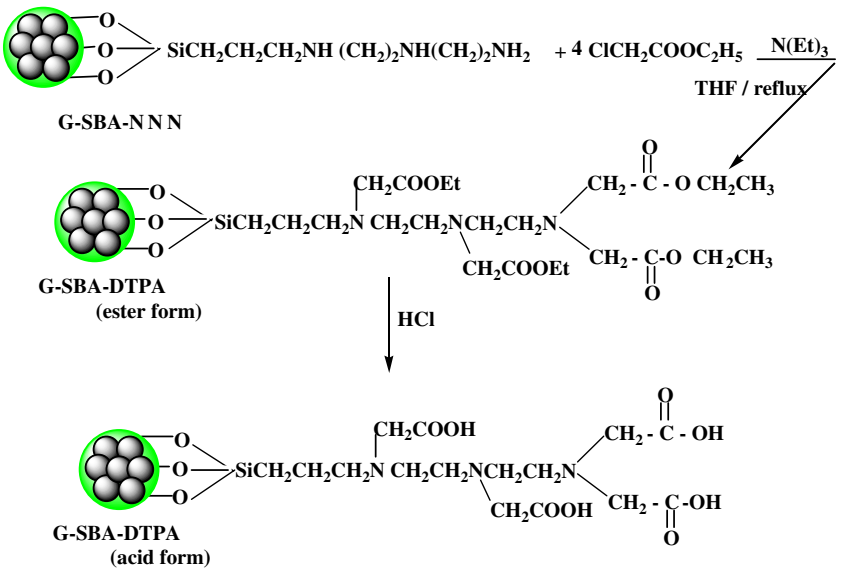

3 Results and Discussions

3.1 Synthesis

Modified mesoporous silica materials G-SBA-IDA, G-SBA-EDTA and G-SBA-DTPA were prepared by treating grafted monoamine- diamine- and triamine-mesoporous silica SBA-15, namely G-SBA-N, G-SBA-NN and G-SBA-NNN with excess ethylchloroacetate. The ester form materials were converted into the corresponding acid form materials using 2M HCl (Schemes 2, 3 and 4). It is confirmed that the acetate groups are covalently bound to the amine nitrogen atoms and that most ester groups were completely converted into the acid form as evident from FTIR, TGA and XPS results. The mesoporous order of materials is maintained after the reaction with ethylchloroacetate, this was evident from TEM and SAXS analysis discussed later.

3.2 XPS Results

Typical survey regions are displayed in Fig. 1 for SBA-15 silica and amine- modified silica (G-SBA-N and G-SBA-NNN), G-SBA-NN was removed from Fig. 1 for simplicity. They exhibit five main peaks: Si2p, Si2s, C1s, N1s and O1s centered at 103, 153, 285, 400 and 533 eV, respectively. On one hand, the SBA-15 silica is free of nitrogen, whilst on the other hand a qualitatively note higher N1s/Si2p intensity ratio on going from G-SBA-N and G-SBA-NNN. Figure 2a and b display N1s narrow regions from

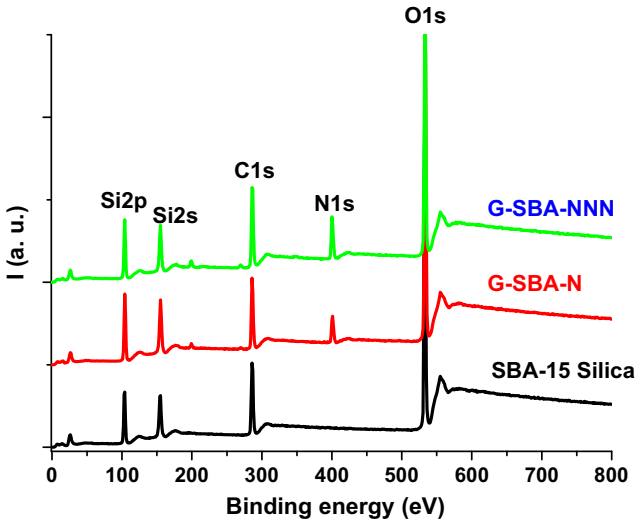

Fig. 1 XPS survey spectra of pristine mesoporous silica, G-SBA-N and G-SBA-NNN

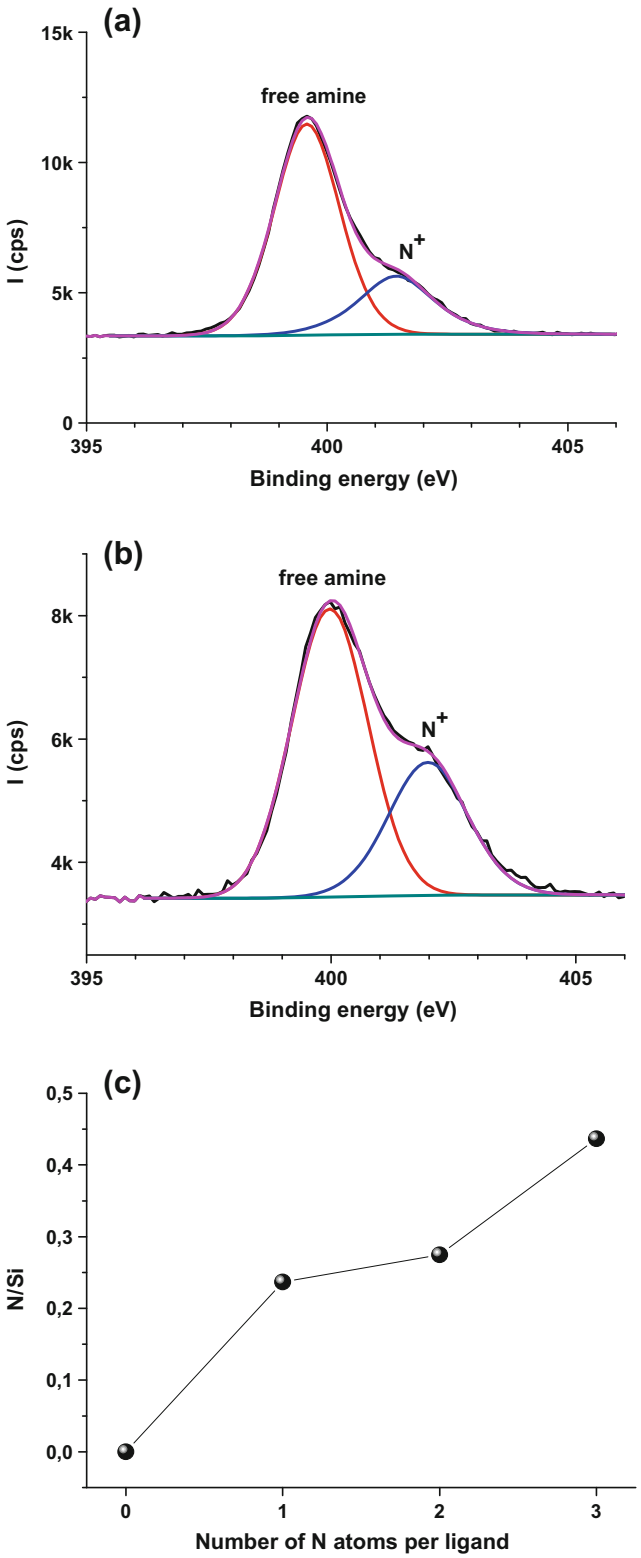

Fig. 2 High resolution, peak-fitted N1s regions from **a** G-SBA-NNN **b** G-SBA-DTPA **c** N/Si atomic ratio versus the number of nitrogen atoms per ligand. The number zero corresponds to pristine silica

G-SBA-NNN before and after attachment of IDA groups, together with the N/Si atomic ratio determined for G-SBA-N, NN and NNN. The N1s peaks have two components centered at ~ 399.6 and 401.5 eV corresponding to free and quaternized amine. Table 1 reports the surface composition of SBA-15 and functionalized mesoporous silica samples.

The extent of carbon increase on going from monoamine to diamine and then to triamine is evident. This accounts for the chemical structures displayed in Schemes 1–3. Similarly, Table 1 and Fig. 2c indicate a progressive increase of the N/Si atomic ratio which accounts for the theoretical number of nitrogen atoms per ligand. Note however that part of the nitrogen atoms are positively charged, most probably quaternized; we invariably observed a higher N^+/N after attachment of the IDA group (see Table 1). Quaternization is due to the HCl hydrolysis. As a matter of fact, we frequently detected chlorides in the powder particle surfaces.

High resolution C1s peaks were fitted with three components centered at 285, ~ 286.5 and ~ 289 eV, assigned to C-C/C-H, C-N/C-O and COOR (R = C or H), respectively. The component in the middle at 286.5 eV is probably composed of two overlapped components of a major C-N and a minor C-O [22]. Note that Fig. 3a exhibits an intense C-O C1s component for silica; this is due to the pluronic employed for the synthesis of mesoporous silica.

Figure 3b and c display the C1s narrow regions for G-SBA-NNN and G-SBA-DTPA, respectively. After attachment of IDA groups, the COOR contribution to the C1s peak area increases significantly. This is invariably observed for all ligand-functionalized meoporous silicas as reported in Table 2. From Tables 1 and 2, we calculated the C_{COOR}/Si atomic ratio (R = H or ethyl) for all grafted silica. The results showed that there is an increasing of C_{COOR}/Si from 2.0 for IDA to 2.7 for EDTA and to 3.2 for DTPA as the number of nitrogen atoms increased. This of course results from increasing the number of IDA ligand sites that could bind with metal ions. Figure 4 brings strong supporting evidence for the significant change in the fine structure of the

Table 1 Surface chemical composition of pristine and modified mesoporous SBA-15 silica samples

Materials	Si	O	C	N	N^+	Cl
SBA-15 Silica	21.3	49.3	29.4			
G-SBA-N	25.0	42.1	26.3	4.46	1.46(24.7%)	0.73
G-SBA-IDA	22.5	43.2	28.6	3.3	1.72(34.3%)	0.70
G-SBA-NN	24.5	43.6	24.8	5.22	1.51(22.4%)	0.39
G-SBA-EDTA	21.9	41.6	29.1	4.94	1.63(24.8%)	0.94
G-SBA-NNN	21.1	37.9	30.87	6.91	2.30(25%)	0.97
G-SBA-DTPA	20.0	39.2	32.6	4.57	2.23(32.8%)	1.40

The numbers between brackets indicate the contribution (in %) of the quaternized nitrogen atoms to the total amount of nitrogen

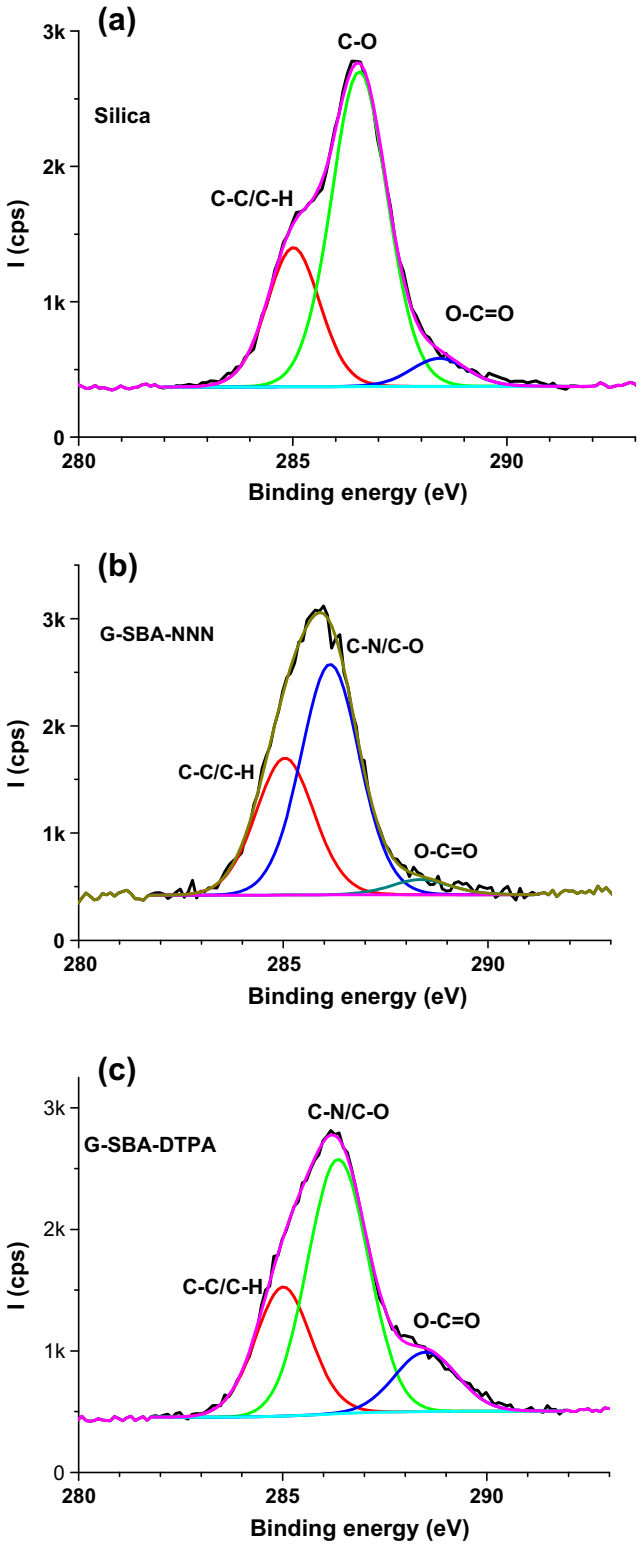

Fig. 3 Peak-fitted narrow C1regions of **a** pristine mesoporous silica, **b** G-SBA-NNN, and **c** G-SBA-DTPA

C1s narrow regions. It follows that one can monitor the subtle change in the chemistry of the mesoporous silica by XPS and can thus verify the change in the chemical structures of

Table 2 Peak fittings parameters for C1s regions

Materials	CC/CH	C-N/C-O	-COOR
SBA-15 Silica	27.3	66.7	6.0
G-SBA-N	62.9	34.0	3.1
G-SBA-IDA	48.1	39.9	12.0
G-SBA-NN	36.4	57.8	5.8
G-SBA-EDTA	31.8	52.1	16.1
G-SBA-NNN	35.8	60.6	3.6
G-SBA-DTPA	27.5	58.5	14.0

the ligands from amine groups (monoamine, diamine and triamine) to the iminodiacetate groups.

3.3 FTIR Spectra

FTIR spectra for mesoporous SBA-15 silica, its modified monoamine G-SBA-N and G-SBA-IDA-ester and acid derivatives are given in Fig. 5a–d. The spectra show three regions of absorption bands at 3500–3300 cm^{-1} due to v(OH) or v(N-H) , 1750 −1550 cm^{-1} due to δ(OH) or δ(NH), v(C=O) or v(CO-N) and at 1200–700 cm^{-1} due to v(Si-O) vibrations of the inorganic backbone (Fig. 5a–d). Peaks at 2943, 2826, 1472 cm^{-1} are due to the C-H vibrations of methylene groups [24–28]. The FTIR spectrum of the SBA-15 (Fig. 5a) showed strong peaks at 3400 and 1640 cm^{-1} due to O-H stretching and bending vibrations respectively. Strong peaks around 1080, 795, 960 cm^{-1} are due to v(Si-O-Si) asymmetrical and symmetrical vibrations and v(Si-O-H) stretching vibrations, respectively. The peak around 960 cm^{-1} corresponds to free non-condensed silanols Si-OH groups for SBA-15 material, which decreases in intensity upon modification of SBA-15 with aminosilane agent (Fig. 5b, G-SBA-N), the two bands at 1640 and 1555 cm^{-1} are associated with δ(O-H) and δ(N-H) respectively for G-SBA-N. The FTIR spectrum of the G-SBA-IDA-ester (Fig. 5c) shows two absorptions at 1742 cm^{-1} and 1626 cm^{-1} due to v(C=O) vibration of the ester group (-COOEt) and OH bending vibration [17–19, 21]. The spectrum of the G-SBA-IDA-acid form ligand system (Fig. 5d) shows a strong absorption at 1670 cm^{-1} due to υ(C=O) vibration and a small shoulder at 1740 cm^{-1} for v(C=O) of the ester group. The presence of a small shoulder at 1740 cm^{-1} after hydrolysis with HCl indicates that not all ester groups (-CH_2COOEt) were converted to the acid form (-CH_2COOH) [18, 19]. These assignments are based on reported spectral FTIR data of similar systems [24–28]. The FTIR spectra for grafted diamine and triamines and their G-SBA-EDTA and G-SBA-DTPA, respectively showed similar patterns as that of SBA-15 and its G-SBA-IDA derivative.

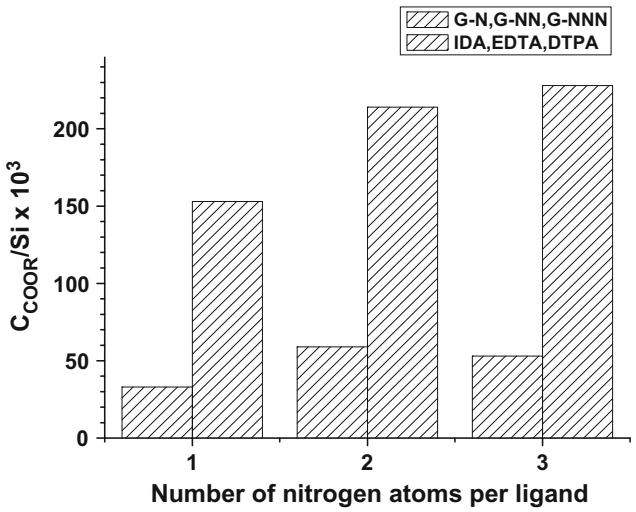

Fig. 4 Plot of C_{COOR}/Si atomic ratio versus the number of nitrogen atoms per ligand. The number zero corresponds to pristine silica

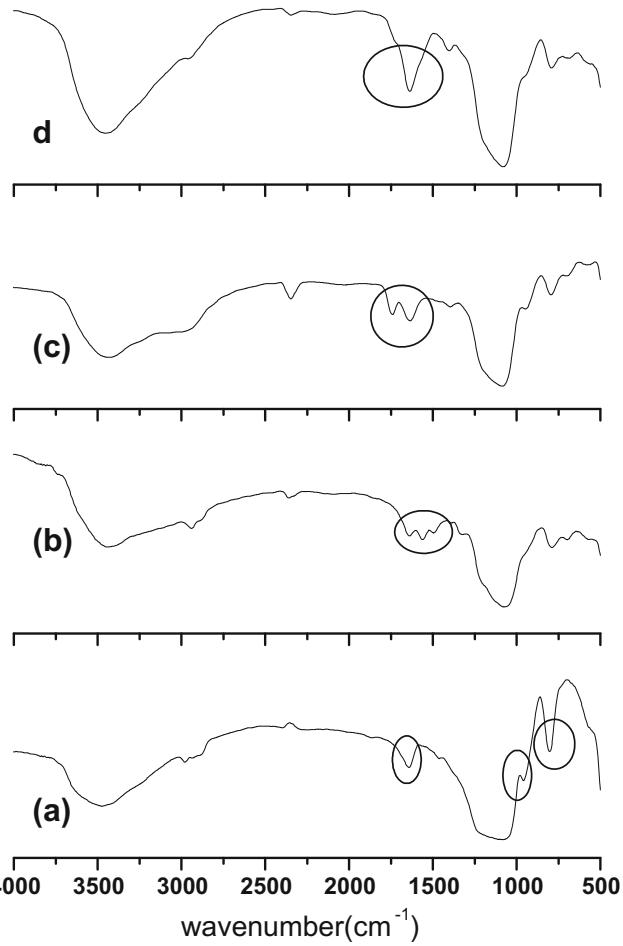

Fig. 5 FTIR spectra of **a** SBA-15, **b** G-SBA-N, **c** G-SBA-IDA ester form, **d** G-SBA-IDA acid form

3.4 TGA Analysis

Thermogravimetric analysis (TGA) and differential thermogravimetric analysis (DTA) for SBA-15 mesoporous silica, grafted monoamine G-SBA-N mesoporous silica and its modified derivative G-SBA-IDA were examined under nitrogen atmosphere at 20–600 °C at a rate of 10 °C/minute. Figure 6a shows the thermogram of SBA-15 material; two peaks were observed, the main preak occurs at ∼75 °C due to loss of 5% of its initial weight. This is attributed to loss of physisorbed water and alcohol from the system pores [17]. The second peak at ∼390 °C, the system loss 16%, is probably due to dehydroxylation and loss of water or alcohol from silica [29–31]. The total loss of weight was 21%. Figure 6b shows the thermogram of G-SBA-N; it also shows two peaks, the main peak occurs at ∼75 °C with a shoulder at 140 °C due to loss of 10% of its initial weight, which is attributed to loss of physisorbed water and alcohol and residual sufactant, respectively from the system pores [18, 23, 29–31]. The second peak occurs at ∼470 °C due to loss of 21% of its initial weight, which is probably due to degradation of organofunctional groups bound to silicon atoms as well as dehydroxylation and loss of water from silica. The total loss of weight was 31%. The thermogram for G-SB-IDA material depicted in Fig. 6c shows three peaks at 80 °C, 300–400 °C and >400 °C. The first peak at 80 °C (3%) is attributed to loss of physisorbed water and alcohol from the system pores. The second peak at the temperature range 300–400 °C is probably due to loss and degradation of organofunctional groups (16.5%) [18, 23].

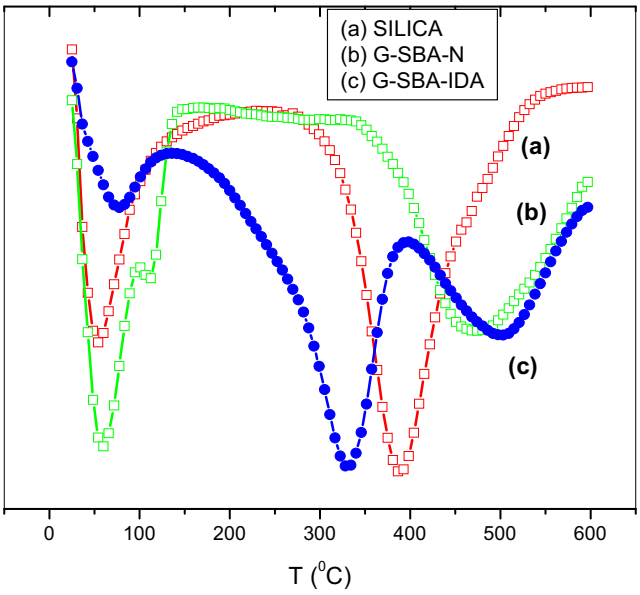

Fig. 6 TGA-DTA thermogram of **a** SBA-15, **b** G-SBA-N, **c** G-SBA-IDA

The third peak at temperature of 400–600 °C is probably due to further condensation of hydroxyl groups from siloxane bonds (dehydroxylation) [29–31]. The increases in weight loss from 21% for G-SBA-15 silica to 31% for G-SBA-N to 33.5% for SBA-IDA silica is consistent with increasing of organic contents in the following order:

SBA-15 > G-SBA-N > G-SBA-IDA

There is no clear correlation between thermal and spectroscopic properties of the functionalized mesoporous system [32].

3.5 BET Analysis

The one-point BET analysis method of adsorption–desorption isotherms at 77 K was used for determination of surface area for all considered materials. Textural properties obtained from the experimental isotherms are given in Table 3. Firstly, the calcinated SBA-15 has high surface area than that of extracted SBA-15 silica(surfactant was washed with ethanol). This is probably due to presence of unremoved surfactant and solvents. Significant reduction of porosity of G-SBA-N, G-SBA-NN and G-SBA-NNN, and their IDA derivatives in comparison with the parent SBA-15 material is evident. This was reflected by the significant drop in the surface area of SBA-15 silica material, after modification [33, 34]. It is obvious that the diamine system has the highest surface area in comparison with that of the monoamine and triamine systems. From the atomic Si/N ratios obtained from the XPS data (Table 1), it is clearly noted that less diamine and triamine groups are grafted into the silica precursor than the monoamine probably due to sterric hindrance reasons. This probably makes the diamine material (which has less steric hindrance than the triamine) exhibit the highest surface area (Table 3). Furthermore, as presented in Table 3, there is further significant decrease in surface area values, after modification by grafted amines with IDA

Table 3 BET specific surface area of SBA-15 silica and its derivatives

Material	Surface area (m^2g^{-1})	d_{100} spacing (nm)	Nitrogen content ($mmolg^{-1}$)
G-SBA-N	170	10.2	0.75(1.9)
G-SBA-IDA	165	9.8	–
G-SBA-NN	256	10.2	1.25(2.77)
G-SBA-EDTA	162	10.0	–
G-SBA-NNN	139	10.8	1.75(3.50)
G-SBA-DTPA	120	9.4	–
SBA-15-extraction	600	9.2	–
SBA-15-calcination	910	8.8	–

groups. The introduction of amine and IDA functional groups onto the internal and the external sides of the pore openings has formed different textural properties from that of the parent SBA-15 mesoporous materials (Table 3).

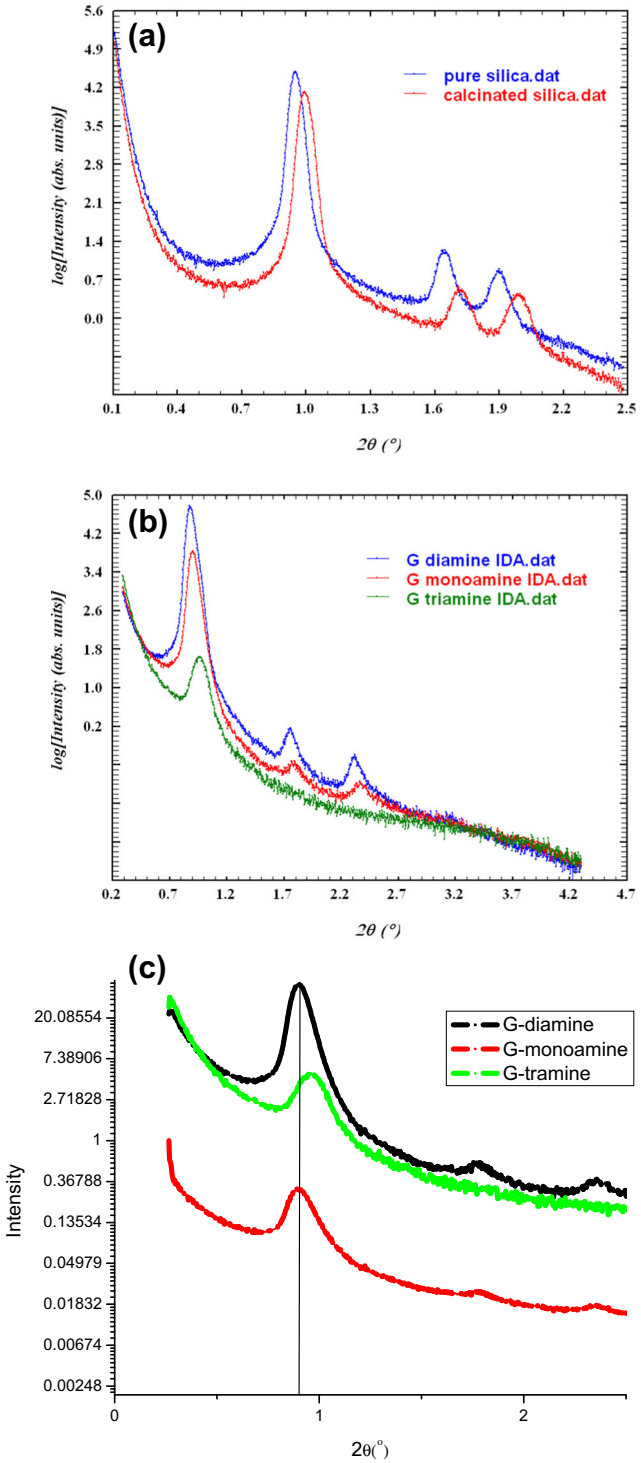

Fig. 7 SAXS analysis of **a** silica and calcinated silica, **b** G-monoamine-IDA(G-SBA-IDA), G-diamine-IDA(G-SBA-EDTA), G-triamine-IDA(G-SBA-DTPA), **c** G-diamine, G-triamine, G-monoamine

3.6 XRD Analysis

Small angle X-ray diffraction (SXRD) patterns of silica SBA-15-extraction and SBA-15-calcinated are presented in Fig. 7a. It shows a typical pattern of a hexagonal phase with the occurrence of three well-resolved diffraction peaks corresponding to the planes indexed to (100), (110) and (200). This is associated with highly ordered mesoporous silica SBA-15 with a two-dimensional hexagonal symmetry (space group p6mm) [35]. There is a slight shift of all three peaks to higher angles for the silica SBA-15-calination in comparison with SBA-15-extraction [36]. The decrease of interplanar spacing (silica contraction) is probably due to further condensation of silanol groups and removal of surfactant and solvents from the pores of SBA-15. The $d_{10}0$ spacing value has decreased from 9.2 nm for silica SBA-15-extraction to 8.8 nm for silica SBA-15-calcination (Table 3). The small angle XRD patterns for IDA-modified ligand systems are given in Fig. 7b. It shows a typical pattern of a hexagonal phase with the occurrence of a strong peak, due to the (100) plane, and another two weak peaks, due to the (110) and (200) planes as shown in Fig. 7a. This confirms that the ordered structure was not particularly affected by the functionalization steps. But in the case of the G-SBA-DTPA system there was a significant decreasing of intensity of the (100) peak and a shift to a larger angle with absence of the other two small peaks (110) and (200); this may imply there was some distortion of mesoporosity of the G-SBA-DTPA material in comparison with that of G-SBA-DTP and G-SBA-DTPA (Fig. 7b). The small angle patterns for the G-monoamine and G-diamine showed similar patterns to that of its parent SBA-15-calcinated (Fig. 7c). But in the case of G-triamine there was a shift of the d_{100} peak to a larger angle with disappearance of the other two small peaks (110 and 200) probably due to distortion of its mesoporosity (Fig. 7c). There is no trend for d_{100} spacing given in Table 3, the values are in the range of 9.0-10.0 nm. There was a shift towards larger d_{100} spacing after functionalization, which is probably reflected by decrease of surface area (Table 3).

3.7 TEM and SEM-EDS Analysis

Figure 8a shows SEM image of high magnification power of G-SBA-EDTA material. It shows well-defined lamellar shape layers of smaller sizes in the range 0.5-1.0 µm (Fig. 8a) than that of the parent SBA-15 silica material (Fig. 9a). The EDX elemental analysis pattern reveals the presence of the main elements Si, O, C and N as evidence for the introduction of ethylchloroacetate groups. The presence of Cl peaks probably comes from the generated HCl from the reaction between chloroethylacetate and amine species (Scheme 2). The mesoporous ordered structure of G-SBA-EDTA material was confirmed from TEM analysis

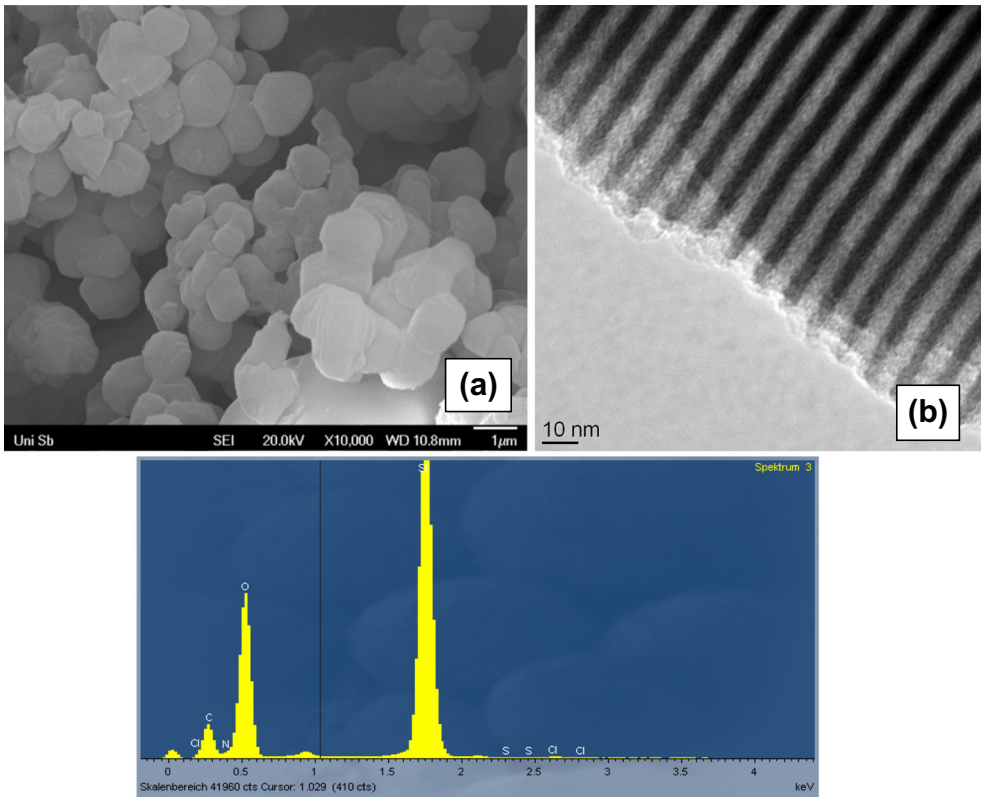

Fig. 8 SEM image of **a** G-SBA-IDA, **b** TEM image of G-SBA-IDA and its EDS

(Fig. 8b). The TEM image of G-SBA-EDTA material shows cylindrical channels taken along the 110 and 100 directions indicating 2D p6mm meostructure [37]. The presence of the mesoporous structure in the final functionalized solid was also confirmed by TEM analysis (Fig. 8b) in which the typical channels of the G-SBA-EDTA matrix are seen as black and white stripes. SEM and TEM images of SBA-15 material (Fig. 9a and b) reveal the presence of lamellar shape layers of different sizes; the EDX analysis pattern shows only the two main elements Si and O of the silica and traces of carbon which may be due to some contamination or unhydrolyzed alkoxy groups. The presence of the mesoporous

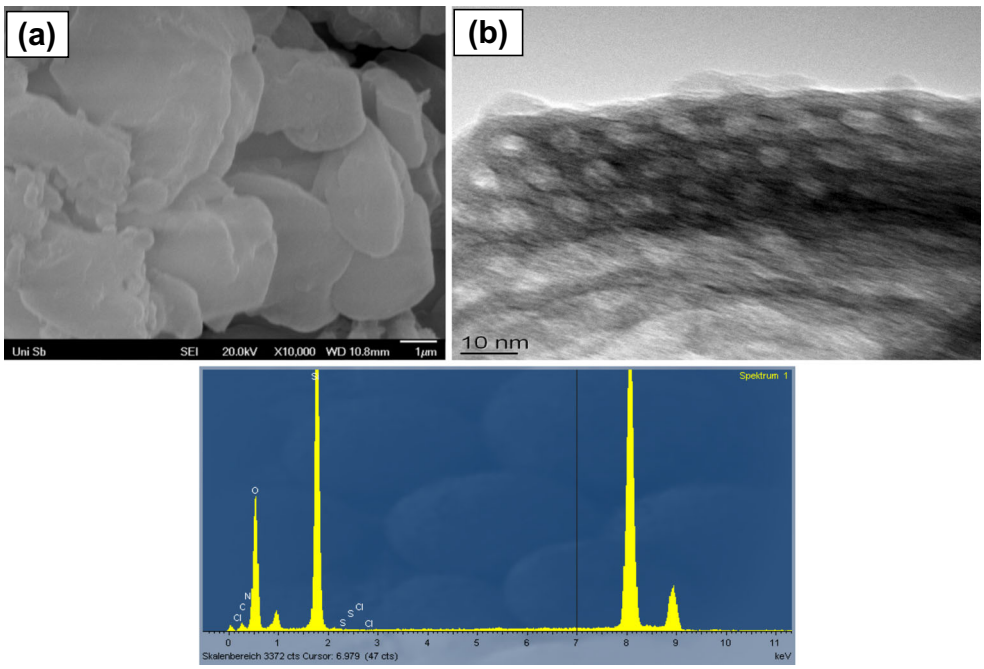

Fig. 9 SEM image of **a** SBA-15, **b** TEM image of SBA-15 and its EDS

structure in the final functionalized solid was also confirmed by TEM analysis (Fig. 9b). The estimated pore diameter is about 5 nm, center to center pore distance is about 10 nm and pore wall thickness is about 5 nm which are very close to reported data [37].

3.8 Metal Uptake Study

A first group of experiments was carried out to test the ability of synthesized materials to act as heavy metal adsorbents; mesoporous silica SBA-15 and functionalized monoamine G-SBA-N and its modified G-SBA-IDA were included. Aqueous solutions of metal ions of each IDA-functionalized adsorbent at 25 °C and the assays were repeated for copper nitrate, lead nitrate, cobalt nitrate and nickel nitrate. SBA-15 silics experiments yield null adsorption at this detection level, so metal loading of the modified SBA-15 samples should exclusively be attributed to the presence of active IDA groups anchored to the silica walls. The metal uptake adsorption study for G-SBA-N, NN and NNN materials was previously reported [17] and is beyond our aim. The metal ion uptake adsorption was determined by a batch method by mixing each of the modified amine IDA derivatives: G-SBA-IDA and G-SBA-EDTA G-SBA-DTPA-modified mesoporous ligand systems with solutions of metal ions (Co^{2+}, Ni^{2+}, $Cu^{2+}$and Pb^{2+}). Measurements were carried out at room temperature after 72 hours uptake time to reach equlibrium. Table 4 reports the maximum metal uptake capacity of the different metal ions (Co^{2+}, Ni^{2+}, $Cu^{2+}$and Pb^{2+}) along with those data of reported similar IDA- and EDTA-functionalized polysiloxane ligand systems. The comparison of IDA, EDTA and DTPA functional groups for the adsorption of metal ions showed no distinct difference between the three systems. The long diffusion channels in mesoporous silicates are considered as the major reason. If so, a comparison for the adsorption ability by the same group modified SBA-15 but with different loadings is recommended.

It is confirmed that the maximum uptake capacities for the three new modified ligand systems (G-SBA-IDA and G-SBA-EDTA and G-SBA-DTPA) are much higher in comparison with similar reported EDTA-modified ligand systems for lead ion [22] and IDA-immobilized ligand system of copper and nickel ions [37]. These differences are probably due to the preparation route and therefore the availability of the ligand sites on the silica network. The results show no significant differences for the metal uptake between the three involved functionalized ligand systems (Table 4) despite the increasing of the number of acetate functional ligand groups. The reason for this is probably that when ligand sites at the pore surface are first involved in complexation with metal ions they may block the accessibility of other ligand sites for complexation to metal ions. The metal uptake capacity of all ligand systems was found to increase in the following order:

$$Co^{2+} < Ni^{2+} < Pb^{2+} < Cu^{2+}$$

The functionality of the IDA group acts as tridentate ligand bonding to metal ions through the imino nitrogen atom and through two carboxylic oxygen atoms through deprotonation [38]. The chelating ligand attached to a silica matrix should possess strong metal binding properties and selectivity toward certain metal ions. According to the hard-soft acid-base (HASB) theory by Pearson [39, 40], the metal ions, for instance, copper(II), nickel(II), cobalt(II) ions, which lie in the border line(intermediate) should have different affinities with donor atoms as O and N of the IDA functional group. Therefore, the anion of IDA is considered as a hard ligand. The adsorption capacity followed the order of Cu(II) > Pb(II) > Ni(II) > Co(II) which is consistent with the hard–soft acid–base theory and is consistent with similar reported systems [18, 41]. The IDA chelating ligand forms mainly 1:1 complexes with different metal ions, though the possibility of 1:2 metal to ligand complexes may occur.

Table 4 Metal uptake capacities (mmol g^{-1}) of materials

Divalent metal ions	G-SBA-IDA $mmolg^{-1}$	G-SBA-EDTA $mmolg^{-1}$	G-SBA-DTPA $mmolg^{-1}$
Copper	2.0(1.23)[19]	2.1(1.56) [35]	2.08
Nickel	1.34(1.1)	1.51(1.5) [35]	1.65
Cobalt	1.2(1.1)	1.12(1.33) [35]	1.11
Lead	1.4	1.34(0.43) [22]	1.5

4 Conclusion

- Functionalized mesoporous SBA-15 silica materials labled G-SBA-IDA. G-SBA-EDTA and G-SBA-DTPA are obtained by modification of monoamine, diamine and triamine-grafted mesoporous SBA-15 material with chloroethylacetate.
- The mesoporous structure of functionalized mesoporous ligand systems is maintained after the modification process and the ethyacetate groups are covalently bound to amine nitrogen atoms of mesoporous silica.
- SAXS and BET confirmed the mesoporous ordered structure was not particularly affected by the functionalization steps, but there was a shift towards larger d_{100} spacing upon amine functionalization, which results in decreasing surface area.
- FTIR spectra showed that the ester functional groups are mostly converted to the acid form upon treatment with HCl.

- The three adsorbents are very efficient even at low metal concentration and substantial amounts of M(II) can be removed from aqueous solutions. Such materials can also be used in several applications not only for extraction, separation and removal of pollutants but also for many other purposes.

Acknowledgments The authors would like to thank the French Government for the Al-Maqdisi grant jointly with the Palestinian Ministry of Higher Education.

Compliance with Ethical Standards

Conflict of interests The authors would like to declare that they have no conflict of interest.

References

1. Lui AM, Hidajat K, Kawi S, Zhao D (2000) A new class of hybrid mesoporous materials with functionalized organic monolayers for selective adsorption of heavy metal ions. Chem Commun 13:1145–1146
2. Hoffmann F, Cornelius M, Morell J, Froeba M (2006) Silica-based mesoporous organic-inorganic hybrid. Mater Angew Chem Int Ed 45:3216–3251
3. Wan Y, Zhao D (2007) On the controllable soft-templating approatch to mesporous silicates. Chem Rev 107:2821–2860
4. Sanchez C, Boissiere C, Grosso D, Laberty C, Nicole L (2008) Synthesis, and properties of inorganic and hybrid thin films having periodically organized nanoporosity. Chem Mater 20:682–737
5. Stein A, Melde BJ, Schroden RC (2000) Hybrid inorganic–organic mesoporous silicates—nanoscopic reactors coming of age. Adv Mater 12:1403–1419
6. Xia K, Ferguson RZ, Losier M, Tchoukanova N, Bruning R, Djaoued Y (2010) Synthesis of hybrid silica materials with tunable pore structures and morphology and their application for heavy metal removal from drinking water. J Hazar Mater 183:554–564
7. Sayari A, Hamoudi S (2001) Periodic mesoporous silica-based organic−inorganic nanocomposite materials. Chem Mater 13: 3151–3168
8. Wahab MA, Kim I, Ha CS (2004) Bridged amine-functionalized mesoporous organosilica materials from 1,2-bis (triethoxysilyl)ethane and bis[(3-trimethoxysilyl)propyl]amine. J Solid State Chem 177:3439–3447
9. Wang X, Tseng TH, Chan JC, Cheng S (2005) Ctalytic application application of ....by a template-free rout in flavanones synthesis. J Catal 233:266–275
10. Lei C, Shin Y, Liu J, Ackerman EJ (2002) Entrapping enzyme in a functionalized nanoporous support. J Am Chem Soc 124:11242–11243
11. Munoz B, Ramila A, Perez-Pariente J, Diaz I, Vallet-Regi M (2003) MCM-41 organic modification as drug delivery rate regulator. Chem Mater 15:500–503
12. Walcarius A, Etienne M, Lebeau B (2003) Rate of access to the binding sites in organically modified silicates. Ordered mesoporous silicas grafted with amine or thiol groups. Chem Mater 11:2161–2173
13. Bartovsky P, Ribes A, Agostini A, Benito A (2014) Deliverymodulation in silicamesoporoussupports via functionalization in theporeoutletswit a Zn(II)-bis(2-pyridylmethyl)aminecomplex. Inorg Chimica Acta 417:263
14. Anspach FB (1994) Silica-based metal chelate affinity sorbents I. Preparation and characterization of iminodiacetic acid affinity sorbents prepared via different immobilization techniques. J Chromatogr A 672:35–49
15. Tikhomirova TI, Lukyanova MV, Fadeeva VI, Kudryavtsev GV, Shpigun OA (1993) Preconcentration of some transition-metals on silica modified by grafted iminodiacetic acid groups. J Anal Chem 48:52–55
16. Sadikova ZA, Tikhomirova T. I., Lapuk A. V., Fadeeva VI (1997) Sorption of vanadium(IV),vanadium(V) and molybdenum (VI) on silia chemically modified with iminodiacetic acid groups. J Anal Chem 52:206–208
17. Gao ZF, Wang L, Qi T, Chu J, Zhang Y (2007) Synthesis, characterization, and cadmium(II) uptake of iminodiacetic acid-modified mesoporous SBA-15, Colloids Surf. A –Physicochem. Eng Aspects 304:77–81
18. El-Ashgar NM, El-Nahhal IM, Chehimi MM, Babonneau F, Livage J (2007) A new route synthesis of immobilized-polysiloxaneiminodiacetic acid ligand system. Its characterization and applications. Mater Lett 614:553–4558
19. El-Nahhal IM, F Zaggout FR, Nassar MA, El-Ashgar NM, Maquet J, Babonneau F, Chehimi MM (2003) Synthesis, Characterization and applications of immobilized iminodiacetic acid-modified silica. J Sol–Gel Sci Technol 28:255
20. Busche B, Wiacek R, Davidson J, Koonsiripaiboon V, Yantasee W, Addleman SR, Fryxell GE (2009) Synthesis of NanoporousIminodiacetic Acid Sorbents for Binding Transition Metals. Inorg Chem Communs 123:312–315
21. El-Nasser AA, Parish RV (1999) Solid polysioxane ligands containing glycinate- or iminodiacetate- groups: Synthesis and application to binding and separation of metal ions. J Chem Soc Dalton Trans: 3463
22. Huang J, Ye M, Qu Y, Chu L, Chen R, He Q, Xu D (2012) Pb (II) removal from aqueous media by EDTA-modified mesoporous silica SBA-15. J Colloid Interf Sci 385:137–146
23. Yoshitake H, Yokoi T, Tatsumi T (2002) Amino-functionalized mesoporous silica as base catalyst and adsorbent, Chem Lett P586
24. Yokoi T, Yoshitake H, Tatsumi T (2004) Synthesis of amino-functionalized MCM-41 via direct co-condensation and post-synthesis grafting methods using mono-, di- and tri-amino-organoalkoxysilanes. J Mater Chem 14:951
25. Chong ASM, Zhao XS (2003) Functionalization of SBA-15 with APTES and characterization of functionalized materials. J Phys Chem B 1071:2650
26. Hiyoshi N, Yogo K, Yashima T (2005) Adsorption characteristics of carbon dioxide on organically functionalized SBA-15 Microporous Mesoporous. Microporous Mesoporous Mater 84: 357–365
27. Diaz JF, Balkus JK, Bedioui F, Kurshev V, Kevan L (1997) Synthesis and characterization of cobalt-complex functionalized MCM-4. Chem Mater 9:61–67
28. Yang SM, Coombs N, Ozin GA (2000) Micromolding in inverted polymer opals (MIPO): Synthesis of hexagonal mesoporous silica opal. Adv Mater 121:940–1944
29. Liu X, Zhou L, Fu X, Sun Y, Su W, Zhou Y (2007) Adsorption of Pb^{2+} and Cu^{2+} on anionic surfactant-templated amino-functionalized mesoporous silicas. Chem Eng Sci 62:1101–1110
30. Huang HY, Yang Daniel Chinn RT, Munson CL (2003) Amine-Grafted MCM-48 and Silica Xerogel as Superior Sorbents for Acidic Gas Removal from Natural Gas. Ind Eng Chem Res 422:427–2433
31. Harlick PJE, Sayari A (2007) Applications of pore-expanded mesoporous silica. Triamine grafted material with exceptional CO_2 dynamic and equilibrium adsorption performance. Ind Eng Chem Res 46:446-458

32. Rocha MVJ, De Carvalho HWP, Sarmento VHV, Craievich AF, Ramalho TC (2016) Structural characterization, thermal properties, and density functional theory studies of pmma-maghemite hybrid material. Polym Compos 37:51–60
33. Ren T, Yuan ZY, Su B (2007) Encapsulation of direct blue dye into mesoporous silica-based materials. Colloids Surf A: Physicochem Eng Asp 300:79–87
34. Hamoudi S, El-Nemr A, Belkacemi K (2010) Adsorptive removal of dihydrogen phosphate ion from aqueous solutions using mono, di- and tri-ammonium-functionalized SBA-15. J Colloid. Interface Sci 343:615
35. Zhao D, Feng J, Huo Q, Melosh N, Frederickson G, Chmelka B, Stucky G (1998) Science 279:548
36. Sareen S, Mutreja V, Singh S, Pal B (2016) Fine CuO anisotropic nanoparticles supported on mesoporous SBA-15 for selective hydrogenation of nitroaromatics. J Colloid Interface Sci 461:203
37. Huang C-H, Chang K-P, Oua H-D, Chiang Y-C, Wang C-F (2011) Adsorption of cationic dyes onto mesoporous silica. Micro Meso Mat 141:102
38. El- Ashgar NM, El-Nahhal IM, Chehimi MM, Babonneau F, Livage J (2009) Preparation of ethylenediaminetriacetic acid silica-gel immobilised ligand system and its application for trace metal analysis in aqueous samples Intern. J Environ Anal 89:1057–1069
39. Pearson GR (1963) Hard and soft acids and bases. J Am Chem Soc 85:3533–3539
40. Martin R (2002) Practical hardness scales for metal ion complexes. Inorg Chim Acta 339:27–33
41. Liu HF, Li L, Ling P, Jing X, Li C, Li A, You X (2011) Interaction mechanism of aqueous heavy metals onto a newly synthesized IDA-chelating resin: Isotherms, thermodynamics and kinetics. Chem Eng J 173:106–114